Supplementary Material: Asymmetry-Based Quantum Backaction Suppression in Quadratic Optomechanics

Vincent Dumont*[1], Hoi-Kwan Lau[2], Aashish A. Clerk[3], and Jack C. Sankey[1]

[1] *Department of Physics, McGill University, Montréal, Québec, Canada*
[2] *Department of Physics, Simon Fraser University, Burnaby, British Columbia, Canada*
[3] *Pritzker School of Molecular Engineering, University of Chicago, Chicago, Illinois, USA*

July 22, 2022

*vincent.dumont@mail.mcgill.ca

Contents

1 Backaction Model

Here we derive the expressions for the quantum radiation pressure force noise (QRFN) in an asymmetric cavity optomechanical system. We begin with the general optical equations of motion, eigenmodes, and quadratic coupling in Sec. 1.1, then focus on geometries having purely quadratic dispersive coupling in Sec. 1.2, showing that asymmetry can lead to a large reduction of force noise in Sec. 1.3 at the optimal membrane position. Finally, we discuss quadratic optical trapping (Sec. 1.4), and quantum nondemolition (QND) mechanical energy measurement Sec. 1.5, both of which benefit from reduced force noise.

1.1 Equations of Motion, Eigenmodes, Dissipation and Optomechanical Coupling

General Equations of Motion: To model the optical dynamics, we first write down the input-output equations of motion [1] for sub-cavity operators $\hat{a}_1$ and $\hat{a}_2$ in the frame rotating at an external drive frequency $\omega_{\rm in}$. These are

$$\begin{pmatrix}\dot{\hat{a}}_1\\ \dot{\hat{a}}_2\end{pmatrix} = -i\tilde{\boldsymbol{H}}\begin{pmatrix}\hat{a}_1\\ \hat{a}_2\end{pmatrix} + \tilde{\boldsymbol{\kappa}}^{\rm ext}\begin{pmatrix}\hat{a}_1^{\rm in}\\ \hat{a}_2^{\rm in}\end{pmatrix} + \tilde{\boldsymbol{\kappa}}^{\rm int}\begin{pmatrix}\delta\hat{a}_1^{\rm int}\\ \delta\hat{a}_2^{\rm int}\end{pmatrix} \tag{1}$$

$$\tilde{\boldsymbol{H}} \equiv \begin{pmatrix}-(\Delta - G_1\Delta x) - i\kappa_1/2 & -J\\ -J & -(\Delta - G_2\Delta x) - i\kappa_2/2\end{pmatrix} \tag{2}$$

$$\tilde{\boldsymbol{\kappa}}_{\rm ext} \equiv \begin{pmatrix}\sqrt{\kappa_1^{\rm ext}} & 0\\ 0 & \sqrt{\kappa_2^{\rm ext}}\end{pmatrix} \tag{3}$$

$$\tilde{\boldsymbol{\kappa}}_{\rm int} \equiv \begin{pmatrix}\sqrt{\kappa_1^{\rm int}} & 0\\ 0 & \sqrt{\kappa_2^{\rm int}}\end{pmatrix}, \tag{4}$$

where $\hat{a}_j^{\rm in}$ is the external drive applied to sub-cavity j, $\kappa_j^{\rm ext}$ is the associated (power) coupling rate, $\kappa_j^{\rm int}$ is the sub-cavity's internal loss rate, $\kappa_j = \kappa_j^{\rm ext} + \kappa_j^{\rm int}$ is the total sub-cavity decay rate, G_j is the sub-cavity's optomechanical coupling, and $\Delta = \omega_{\rm in} - \omega_0$ is the drive's detuning relative to the frequency ω_0 at which modes $\hat{a}_1$ and $\hat{a}_2$ are degenerate, which we define to occur at mechanical displacement $\Delta x \equiv 0$.

Optical Eigenmodes: The system's eigenfrequencies

$$\omega_\pm(\Delta x) = \omega_0 + \frac{G_2 + G_1}{2}\Delta x \mp \sqrt{\left(\frac{G_2 - G_1}{2}\Delta x\right)^2 + J^2}, \tag{5}$$

are obtained by diagonalizing the Heisenberg equations of motion ($\dot{\hat{a}}_j = -\frac{i}{\hbar}[\hat{a}, \hat{H}_{\rm opt}]$), and have associated eigenmodes that can be written succinctly as

$$\hat{a}_\pm(\Delta x) = \hat{a}_1\cos(\theta_\pm[\Delta x]) + \hat{a}_2\sin(\theta_\pm[\Delta x]), \tag{6}$$

where the amplitudes satisfy

$$\cot(2\theta_\pm[\Delta x]) = \pm\frac{G_2 - G_1}{2J}\Delta x. \tag{7}$$

Dispersive Couplings: When $G_1 \neq G_2$, the eigenfrequencies of Eq. 5 exhibit an avoided crossing structure, with linear dispersive coupling (LDC)

$$\frac{\partial\omega_\pm(\Delta x)}{\partial x} = \frac{G_1+G_2}{2} \mp \frac{(G_1-G_2)^2}{2\sqrt{4J^2+\left[(G_1-G_2)\Delta x\right]^2}}\Delta x \tag{8}$$

which, if $G_1 < 0$ and $G_2 > 0$, becomes zero at "quadratic points"

$$\Delta x_\pm = \pm\frac{J(G_2+G_1)}{(G_2-G_1)\sqrt{-G_1G_2}}. \tag{9}$$

The frequencies at these extrema are

$$\omega_\pm(\Delta x_\pm) = \omega_0 \mp 2J\frac{\sqrt{-G_1G_2}}{G_2-G_1}, \tag{10}$$

corresponding to an avoided gap $4J\sqrt{-G_1G_2}/(G_2-G_1)$. The quadratic dispersive coupling is generally

$$\frac{\partial^2\omega_\pm(\Delta x)}{\partial x^2} = \mp\frac{2J^2(G_1-G_2)^2}{\left(4J^2+\left[(G_1-G_2)\Delta x\right]^2\right)^{3/2}}, \tag{11}$$

which, at $\Delta x_\pm$, simplifies to

$$\left.\frac{\partial^2\omega_\pm}{\partial x^2}\right|_{\Delta x=\Delta x_\pm} = \mp 2\frac{1}{J}\frac{(-G_1G_2)^{3/2}}{G_2-G_1}. \tag{12}$$

The expressions (as with others involving G_j and J in this document) still represent a general system with two optical modes linearly coupled to one mechanical mode. For a membrane in a cavity, where $G_j = (-1)^j\omega_0/L_j$ and $J = c|t_m|/2\sqrt{L_1L_2}$ (see Appendix 2), with sub-cavity length L_j and membrane (amplitude) transmission t_m, this becomes

$$\left.\frac{\partial^2\omega_\pm}{\partial x^2}\right|_{\Delta x=\Delta x_\pm} = \mp\frac{4}{|t_m|}\frac{\omega_0^2}{cL}, \tag{13}$$

where $L = L_1 + L_2$ is the total cavity length.

Eigenmode Decay Rates: Combined with the sub-cavity (power) losses $\kappa_j = \kappa_j^{\text{int}} + \kappa_j^{\text{ext}}$ (note these exclude J), the amplitudes attached to $\hat{a}_1$ and $\hat{a}_2$ in Eq. 6 permit the calculation of power decay rates

$$\kappa_\pm(\Delta x) = \kappa_1\cos^2(\theta_\pm[\Delta x]) + \kappa_2\sin^2(\theta_\pm[\Delta x]). \tag{14}$$

$$= \bar{\kappa} \mp \frac{(G_1-G_2)\Delta x}{\sqrt{4J^2+\left[(G_2-G_1)\Delta x\right]^2}}\Delta\kappa, \tag{15}$$

for eigenmodes $\hat{a}_\pm$, where $\bar{\kappa} \equiv (\kappa_1 + \kappa_2)/2$ and $\Delta\kappa \equiv (\kappa_1 - \kappa_2)/2$. At the quadratic points,

$$\kappa_\pm(\Delta x_+) = \bar{\kappa} \pm \Delta\kappa \frac{G_2 + G_1}{G_2 - G_1} \tag{16}$$

$$\kappa_\pm(\Delta x_-) = \bar{\kappa} \mp \Delta\kappa \frac{G_2 + G_1}{G_2 - G_1}. \tag{17}$$

For the case of a membrane-cavity system, we can write these (choosing Δx_+) in terms of the end mirror total losses $\mathcal{T}_j = |t_j|^2 + \mathcal{L}_j$ comprising power transmissions $|t_j|^2$ and sub-cavity round-trip power losses $\mathcal{L}_j$:

$$\kappa_+(\Delta x_+) = \frac{c}{2L}(\mathcal{T}_1 + \mathcal{T}_2) \equiv \kappa_0 \tag{18}$$

$$\kappa_-(\Delta x_+) = \frac{c}{2L}\frac{L_2^2\mathcal{T}_1 + L_1^2\mathcal{T}_2}{L_1 L_2}, \tag{19}$$

where we have used $\kappa_j^{\text{int}} = c\mathcal{L}_j/2L_j$ and $\kappa_j^{\text{ext}} = c|t_j|^2/2L_j$. At this location, κ_+ is identical to the empty cavity decay rate κ_0 due to the fact that sub-cavity circulating powers are identical. This is true for any quadratic point we choose.

Dissipative Coupling: From Eq. 14, the linear *dissipative* coupling is

$$\partial_x\kappa_\pm(\Delta x) = \mp 4J^2 \frac{(G_1 - G_2)\Delta\kappa}{\left(4J^2 + [(G_2 - G_1)\Delta x]^2\right)^{3/2}}, \tag{20}$$

which, at the quadratic point, becomes

$$\partial_x\kappa_\pm(\Delta x_\pm) = \pm 4\frac{\Delta\kappa}{J}\frac{(-G_1G_2)^{3/2}}{(G_2 - G_1)^2}, \tag{21}$$

with corresponding single-photon strong coupling parameter

$$\tilde{B}_\pm(\Delta x_\pm) \equiv x_{\text{ZPF}} \left.\frac{\partial_x\kappa_\pm}{\kappa_\pm}\right|_{\Delta x = \Delta x_\pm} = \pm 2\frac{1}{J}\frac{(-G_1G_2)^{3/2}}{G_2(G_2 - G_1)}x_{\text{ZPF}} \tag{22}$$

in the single-port limit ($\kappa_2 \to 0$). We can now see that this coupling can be greatly reduced in the limit $|G_2| \gg |G_1|$. For a single-port membrane-cavity, e.g.,

$$\tilde{B}_\pm(\Delta x_\pm) \to \pm\frac{4}{|t_m|}\frac{\omega_0}{c}\frac{L_2}{L}x_{\text{ZPF}}, \tag{23}$$

which diminishes as L_2/L, suggesting a commensurate reduction of QRFN achieved by simply moving the membrane toward the back mirror.

Equations of Motion at Quadratic Point: Finally, we write down the equations of motion for the eigenmodes $\hat{a}_\pm$ themselves at a quadratic point $\Delta x = \Delta x_+$. First, defining

$$\alpha \equiv \sin(\theta_+[\Delta x_+]) = \cos(\theta_-[\Delta x_+]) = (1 - G_2/G_1)^{-1/2} \tag{24}$$

$$\beta \equiv \cos(\theta_+[\Delta x_+]) = -\sin(\theta_-[\Delta x_+]) = (1 - G_1/G_2)^{-1/2}. \tag{25}$$

for convenience, the equations of motion in the eigenmode basis (Eqs. 1 and 6) become

$$\begin{aligned}\dot{\hat{a}}_+ =& -\left(-i\delta_+ + \frac{\kappa_1}{2}\beta^2 + \frac{\kappa_2}{2}\alpha^2\right)\hat{a}_+ - \alpha\beta\Delta\kappa\hat{a}_- \\ &+ \beta\sqrt{\kappa_1^{\text{ext}}}\hat{a}_1^{\text{in}} + \alpha\sqrt{\kappa_2^{\text{ext}}}\hat{a}_2^{\text{in}} + \beta\sqrt{\kappa_1^{\text{int}}}\hat{a}_1^{\text{int}} + \alpha\sqrt{\kappa_2^{\text{int}}}\hat{a}_2^{\text{int}} \qquad (26)\\ \dot{\hat{a}}_- =& -\left(-i\delta_+ + \frac{\kappa_1}{2}\alpha^2 + \frac{\kappa_2}{2}\beta^2 + i\frac{1}{\alpha\beta}J\right)\hat{a}_- - \alpha\beta\Delta\kappa\hat{a}_+ \\ &+ \alpha\sqrt{\kappa_1^{\text{ext}}}\hat{a}_1^{\text{in}} - \beta\sqrt{\kappa_2^{\text{ext}}}\hat{a}_2^{\text{in}} + \alpha\sqrt{\kappa_1^{\text{int}}}\hat{a}_1^{\text{int}} - \beta\sqrt{\kappa_2^{\text{int}}}\hat{a}_2^{\text{int}}, \qquad (27)\end{aligned}$$

where $\delta_+ \equiv \omega_{\text{in}} - \omega_+ = \Delta + 2J\alpha\beta$ is the detuning from the "+" resonance, and $\Delta\kappa \equiv (\kappa_1 - \kappa_2)/2$ (as above). These reduce to those of Ref. [2] when $|G_1| = |G_2|$, or, equivalently, when $\alpha = \beta = 1/2$. On the other hand, for highly asymmetric coupling $|G_2| \gg |G_1|$ ($|G_1| \gg |G_2|$), we find $\beta \to 1$ and $\alpha \to 0$ ($\alpha \to 1$ and $\beta \to 0$), such that the eigenmodes effectively decouple from one of the inputs, a behavior of central importance in suppressing measurement backaction.

1.2 Measurement Backaction with Quadratic Dispersive Coupling

Optical Susceptibilities: In the frequency domain, the equations of motion in the original sub-cavity basis $\hat{a}_j$ (Eq. 1) can be written

$$\begin{pmatrix}\hat{a}_1(\omega)\\ \hat{a}_2(\omega)\end{pmatrix} = (-i\omega\boldsymbol{I} + i\tilde{\boldsymbol{H}})^{-1}\left[\tilde{\boldsymbol{\kappa}}^{\text{ext}}\begin{pmatrix}\hat{a}_1^{\text{in}}(\omega)\\ \hat{a}_2^{\text{in}}(\omega)\end{pmatrix} + \tilde{\boldsymbol{\kappa}}^{\text{int}}\begin{pmatrix}\delta\hat{a}_1^{\text{int}}(\omega)\\ \delta\hat{a}_2^{\text{int}}(\omega)\end{pmatrix}\right], \qquad (28)$$

where $\boldsymbol{I}$ is the identity matrix, and $\hat{a}_j^{\text{in}}$ comprises any drive and / or fluctuations (including thermal). We can define a susceptibility matrix

$$\begin{aligned}\tilde{\boldsymbol{\chi}}(\omega) &= (-i\omega\boldsymbol{I} + i\tilde{\boldsymbol{H}})^{-1} \\ &= \frac{1}{\chi_1^{-1}(\omega)\chi_2^{-1}(\omega) + J^2}\begin{pmatrix}\chi_2^{-1}(\omega) & iJ\\ iJ & \chi_1^{-1}(\omega)\end{pmatrix} \qquad (29)\\ &\equiv \begin{pmatrix}\tilde{\chi}_{11}(\omega) & \tilde{\chi}_{12}(\omega)\\ \tilde{\chi}_{21}(\omega) & \tilde{\chi}_{22}(\omega)\end{pmatrix}\end{aligned}$$

where

$$\chi_j^{-1}(\omega) = -i(\Delta - G_j\Delta x + \omega) + \kappa_j/2 \qquad (30)$$

is the optical susceptibility of the uncoupled ($J = 0$) sub-cavity j, and $\tilde{\chi}_{ij}$ is shorthand notation for the matrix elements. At the quadratic point $\Delta x = \Delta x_+$, the sub-cavity susceptibilities become

$$\chi_1^{-1}(\omega) = -i\left(\delta_+ - J\alpha/\beta + \omega\right) + \kappa_1/2 \qquad (31)$$

$$\chi_2^{-1}(\omega) = -i\left(\delta_+ - J\beta/\alpha + \omega\right) + \kappa_2/2. \qquad (32)$$

Radiation Force Noise: At the quadratic point Δx_+, the optical force operator $\hat{F}_{\text{opt}} = -d\hat{H}_{\text{opt}}/dx$ reduces to

$$\hat{F}_{\text{opt}}(t) = -\hbar\left(G_1\hat{a}_1^\dagger(t)\hat{a}_1(t) + G_2\hat{a}_2^\dagger(t)\hat{a}_2(t)\right). \qquad (33)$$

The corresponding power spectral density can be written as [1][1]

$$S_{FF}(\omega) = \frac{1}{2\pi}\int_{-\infty}^{\infty} \left\langle \delta\hat{F}^{\dagger}_{\rm opt}(\omega)\delta\hat{F}_{\rm opt}(\omega')\right\rangle d\omega', \tag{34}$$

where $\delta\hat{F}_{\rm opt}(\omega)$ is the Fourier transform of the fluctuations $\delta\hat{F}_{\rm opt}(t) \equiv \hat{F}_{\rm opt}(t) - \langle F_{\rm opt}\rangle$ about the mean (i.e. time-averaged) $\langle F_{\rm opt}\rangle$. Similarly, expressing $\hat{a}_j(t) = \bar{a}_j + \delta\hat{a}_j(t)$ in terms of fluctuations $\delta\hat{a}_j(t)$ about the mean $\bar{a}_j$, we can linearize the optical force operator for small $\delta\hat{a}_j$, yielding

$$\delta\hat{F}_{\rm opt}(t) \approx -\hbar\left(G_1\bar{a}_1^*\delta\hat{a}_1(t) + G_2\bar{a}_2^*\delta\hat{a}_2(t)\right) + \text{c.c.}, \tag{35}$$

such that (similar to Ref. [2]) its Fourier transform becomes

$$\begin{aligned}\delta\hat{F}_{\rm opt}(\omega) = \sum_{j=1,2}\Big(&\sqrt{\kappa_j^{\rm ext}}\mathcal{A}_j(\omega)\delta\hat{a}_j^{\rm in}(\omega) + \sqrt{\kappa_j^{\rm ext}}\mathcal{A}_j^*(-\omega)\delta\hat{a}_j^{\rm in,\dagger}(\omega)\\ &+ \sqrt{\kappa_j^{\rm int}}\mathcal{A}_j(\omega)\delta\hat{a}_j^{\rm int}(\omega) + \sqrt{\kappa_l^{\rm int}}\mathcal{A}_j^*(-\omega)\delta\hat{a}_j^{\rm int,\dagger}(\omega)\Big)\end{aligned} \tag{36}$$

with coefficients

$$\mathcal{A}_1 = -\hbar\left(G_1\tilde{\chi}_{11}(\omega)\bar{a}_1^* + G_2\tilde{\chi}_{21}(\omega)\bar{a}_2^*\right) \tag{37}$$

$$\mathcal{A}_2 = -\hbar\left(G_1\tilde{\chi}_{12}(\omega)\bar{a}_1^* + G_2\tilde{\chi}_{22}(\omega)\bar{a}_2^*\right), \tag{38}$$

where $\tilde{\chi}_{nm}$ are the matrix elements of the optical susceptibility $\tilde{\boldsymbol{\chi}}$ (Eq. 29). Assuming the usual input noise correlators [1]

$$\langle\delta\hat{a}_i^{\rm in}(\omega)\delta\hat{a}_j^{\rm in}(\omega')\rangle = \langle\delta\hat{a}_i^{\rm in,\dagger}(\omega)\delta\hat{a}_j^{\rm in,\dagger}(\omega')\rangle = 0 \tag{39}$$

$$\langle\delta\hat{a}_i^{\rm in}(\omega)\delta\hat{a}_j^{\rm in,\dagger}(\omega')\rangle = 2\pi\delta_{ij}\delta(\omega+\omega')(\bar{n}_j^{\rm in}+1) \tag{40}$$

$$\langle\delta\hat{a}_i^{\rm in,\dagger}(\omega)\delta\hat{a}_j^{\rm in}(\omega')\rangle = 2\pi\delta_{ij}\delta(\omega+\omega')(\bar{n}_j^{\rm in}), \tag{41}$$

where $\bar{n}_j^{\rm in}$ is the mean thermal occupation of the input port bath; the same relations hold for the noise operators of the loss channels by changing subscript "in" $\rightarrow$ "int" throughout (though these ports are considered purely thermal). If the baths are in their ground state ($\bar{n}_j^{\rm in} = \bar{n}_j^{\rm int} \approx 0$), the force noise simplifies to

$$S_{FF}(\omega) = \kappa_1|\mathcal{A}_1(\omega)|^2 + \kappa_2|\mathcal{A}_2(\omega)|^2. \tag{42}$$

In this work, we are particularly interested in the force noise when one eigenmode, having purely quadratic dispersive coupling, is driven by a single port. For example, if

[1] We use the Fourier transform convention $X(\omega) = \int_{-\infty}^{\infty} e^{+i\omega t}X(t)dt$ and $X(t) = \frac{1}{2\pi}\int_{-\infty}^{\infty} e^{-i\omega t}X(\omega)d\omega$, defining $X^{\dagger}(\omega) \equiv \int_{-\infty}^{\infty} e^{+i\omega t}X^{\dagger}(t)dt$; thus, $X^{\dagger}(\omega)$ refers to the Fourier transform of the time domain variable $X^{\dagger}(t)$. Note also that $X^{\dagger}(\omega) = [X(-\omega)]^{\dagger}$ in this convention.

$\Delta x = \Delta x_+$ and the system is driven by $\bar{a}_1^{\text{in}}$ (with $\bar{a}_2^{\text{in}} = 0$), the steady-state amplitudes simplify to

$$\bar{a}_1 = \tilde{\chi}_{11}(0)\sqrt{\kappa_1^{\text{ext}}}\bar{a}_1^{\text{in}} \tag{43}$$

$$\bar{a}_2 = \tilde{\chi}_{21}(0)\sqrt{\kappa_1^{\text{ext}}}\bar{a}_1^{\text{in}}. \tag{44}$$

Together with Eq. 6, the ratio $\bar{a}_1/\bar{a}_2$ now allows us to express $\bar{a}_j$ in terms of $\bar{a}_+$ as

$$\bar{a}_1 = \frac{1}{\beta + i\alpha J\chi_2(0)}\bar{a}_+ \tag{45}$$

$$\bar{a}_2 = \frac{iJ\chi_2(0)}{\beta + i\alpha J\chi_2(0)}\bar{a}_+, \tag{46}$$

which, finally, allows us to write the force noise (Eq. 42) in terms of $|\bar{a}_+|^2$:

$$S_{FF}(\omega) = \hbar^2|\bar{a}_+|^2\frac{1}{|\beta + i\alpha J\chi_2(0)|^2}\Big(\kappa_1\left|G_1\tilde{\chi}_{11}(\omega) - iG_2J\chi_2^*(0)\tilde{\chi}_{21}(\omega)\right|^2 + \kappa_2\left|G_1\tilde{\chi}_{12}(\omega) - iG_2J\chi_2^*(0)\tilde{\chi}_{22}(\omega)\right|^2\Big). \tag{47}$$

In the large-gap limit, where $4J\alpha\beta \gg \kappa_1$, κ_2, $|\omega|$, $|\delta_+|$, such that only the "+" mode is involved, at zero detuning this simplifies to

$$S_{FF}(\omega) = \hbar^2|\bar{a}_+|^2\frac{G_1^2G_2}{4J^2(G_2 - G_1)^2}\frac{4\omega^2G_2\kappa_- + (G_2 - G_1)\kappa_+^2\kappa_2}{\omega^2 + \kappa_+^2/4}. \tag{48}$$

If we instead consider a single-port cavity ($\kappa_2 = 0$ and $\kappa_1 = \kappa_1^{\text{ext}}$), Eq. 47 becomes

$$S_{FF}(\omega) = \hbar^2|\bar{a}_+|^2\frac{\kappa_1^{\text{ext}}}{|\beta + i\alpha J\chi_2(0)|^2}\left|\frac{G_1\chi_2^{-1}(\omega) + G_2J^2\chi_2^*(0)}{\chi_1^{-1}(\omega)\chi_2^{-1}(\omega) + J^2}\right|^2, \tag{49}$$

which reduces to

$$S_{FF}(\omega) = \frac{-\hbar^2|\bar{a}_+|^2\kappa_+G_1^3G_2}{J^2(G_2 - G_1)^2}\frac{(2\delta_+ + \omega)^2}{(\delta_+ + \omega)^2 + \kappa_+^2/4} \tag{50}$$

in the large-gap limit. This expression agrees with the force noise calculated from the simple assumption of dissipative coupling [3] when $\tilde{B}$ is given by Eq. 22.

1.3 Force Noise Reduction

To see how asymmetric sub-cavity LDC can reduce quantum radiation force noise (QRFN), we now consider a membrane-cavity style system. In the large-gap limit, the QRFN (Eq. 49) is

$$S_{FF}(\omega) = \frac{\hbar^2|\bar{a}_+|^2\omega_0^2}{c^2|t_m|^2}\frac{L_2}{L^2}\frac{4L_1\kappa_-\omega^2 + L\kappa_+^2\kappa_2}{\omega^2 + \kappa_+^2/4}, \tag{51}$$

with decay rates

$$\kappa_+ = \frac{L_1}{L}\kappa_1 + \frac{L_2}{L}\kappa_2 \tag{52}$$

$$\kappa_- = \frac{L_2}{L}\kappa_1 + \frac{L_1}{L}\kappa_2, \tag{53}$$

at the quadratic point Δx_+. At the mechanical frequency Ω_m, this be rewritten

$$S_{FF}(\Omega_m) = 4\frac{\hbar^2|\bar{a}_+|^2\omega_0^2}{c^2|t_m|^2}\frac{L_1L_2}{L^2}\kappa_-\frac{L\kappa_2/(L_1\kappa_-) + 4\Omega_m^2/\kappa_+^2}{1+4\Omega_m^2/\kappa_+^2}. \tag{54}$$

This expression can be minimized with respect to L_1 for fixed cavity length, by substituting the expressions for the decay rates (Eqs. 18 and 19), yielding

$$S_{FF}^{\min}(\Omega_m) = 2\frac{\hbar^2|\bar{a}_+|^2\omega_0^2}{cL|t_m|^2}\mathcal{T}_2\frac{1+4\mathcal{B}\Omega_m^2/\kappa_+^2}{1+4\Omega_m^2/\kappa_+^2}, \tag{55}$$

where we defined

$$\mathcal{B} \equiv \frac{\mathcal{T}_1}{\mathcal{T}_1+\mathcal{T}_2}, \tag{56}$$

noting $\mathcal{B} \in [0,1]$ with $\mathcal{B}=1$ corresponding to the "single-port" limit, where $\mathcal{T}_1 \gg \mathcal{T}_2$. This minimum is found a distance

$$L_{1,\min} = \mathcal{B}L \tag{57}$$

from the input mirror.

Modified resolved-sideband limit: In the limit $\Omega_m/\kappa_+ \gg \sqrt{L\kappa_2/4L_1\kappa_-}$ and $\Omega_m/\kappa_+ \gg 1/2$ – both of which are succinctly captured by $\sqrt{\mathcal{B}}\Omega_m \gg \kappa_+$ at $L_{1,\min}$ – the minimal QRFN reduces to

$$S_{FF}^{\min,\mathrm{RS}}(\Omega_m) = 2\frac{\hbar^2|\bar{a}_+|^2\omega_0^2}{cL|t_m|^2}\mathcal{B}\mathcal{T}_2 \tag{58}$$

$$\xrightarrow{\text{Single-Port}} 2\frac{\hbar^2|\bar{a}_+|^2\omega_0^2}{cL|t_m|^2}\mathcal{T}_2, \tag{59}$$

where the second line is evaluated for small but finite $\mathcal{T}_2 \ll \mathcal{T}_1$ ($\mathcal{B} \approx 1$). In the latter case, the QRFN is limited simply by the distance between the lossless back mirror and its closest quadratic point (wavelength scale).

"Modified" fast-cavity limit: In the limit $\Omega_m/\kappa_+ \ll \sqrt{L\kappa_2/4L_1\kappa_-}$ (and $\Omega_m/\kappa_+ \ll 1/2$) – captured succinctly by $\Omega_m \ll \kappa_+$ at $L_{1,\min}$ – the minimal QRFN reduces to

$$S_{FF}^{\min,\mathrm{FC}}(\Omega_m) = 2\frac{\hbar^2|\bar{a}_+|^2\omega_0^2}{cL|t_m|^2}\mathcal{T}_2. \tag{60}$$

which is a factor

$$\frac{S_{FF}^{\min,\mathrm{FC}}(\Omega_m)}{S_{FF}^{\min,\mathrm{RS}}(\Omega_m)} = \frac{1}{\mathcal{B}} \geq 1 \tag{61}$$

larger than that of the resolved-sideband case.

1.4 Application: Optical Trapping

The optical spring generated at a quadratic point has the same strength as a free-space trap [4] per watt incident on the membrane, though with significantly less input power due to the cavity enhancement. As discussed below, our scheme realizes this with lower QRFN than can be achieved in free space (or with a MIM system).

If we write the optical Hamiltonian in the "+" mode basis, and expand its frequency ω_+ to second order in mechanical displacement $\hat{x}$, we find

$$\hat{H}_{\rm opt} = \hbar\omega_+(x)\hat{a}_+^\dagger\hat{a}_+ \approx \hbar\left(\omega_+(0) + \frac{1}{2}\frac{\partial^2\omega_+}{\partial x^2}\hat{x}^2\right)\hat{a}_+^\dagger\hat{a}_+, \tag{62}$$

which allows us to directly identify the spring constant

$$k_{\rm opt} = \hbar\frac{\partial^2\omega_+}{\partial x^2}|\bar{a}_+|^2 = \frac{4}{|t_m|}\frac{\hbar\omega_0^2}{cL}|\bar{a}_+|^2, \tag{63}$$

where we have substituted in the quadratic dispersive coupling $\partial_x^2\omega_+$ from Eq. 13 and considered (for the time being) only the non-dynamical part of the spring (i.e., $\hat{a}_+ \approx \bar{a}_+$). The optical spring can then be expressed as a function of the (mean) circulating power

$$\bar{P}_{\rm circ} = \hbar\omega_{\rm in}\frac{c}{2L}|\bar{a}_+|^2 \tag{64}$$

as

$$k_{\rm opt} = \frac{8}{|t_m|}\frac{\omega_{\rm in}P_{\rm circ}}{c^2}, \tag{65}$$

using $\omega_{\rm in} \approx \omega_0$, which is the same expression as for a free-space trap with a retro-reflected beam [4].

When approaching the single-port limit ($\mathcal{T}_2 \ll \mathcal{T}_1$), the minimal force noise at the optimal membrane position is

$$S_{FF}^{\rm min}(\Omega_m) = \frac{S_{FF}^{\rm FS}}{2}\frac{\mathcal{T}_2}{|t_m|^2}, \tag{66}$$

regardless of whether the system is sideband-resolved, where

$$S_{FF}^{\rm FS} \approx 8\frac{\hbar\omega_{\rm in}}{c^2}\bar{P}_{\rm circ}, \tag{67}$$

is the force noise associated with a free-space trap in the limit $|t_m|^2 \ll 1$. $S_{FF}^{\rm FS}$ can be obtained noting that, for a highly reflective membrane, the force applied to each side is $F \approx 2P_{\rm circ}/c$, yielding a force noise of $S_{FF} = 4S_{P_{\rm circ}P_{\rm circ}}/c^2$. For shot noise, the power spectral density is $S_{P_{\rm circ}P_{\rm circ}} = \hbar\omega_{\rm in}\bar{P}_{\rm circ}$ and since shot noise is uncorrelated at each side of the membrane, it adds in quadrature, yielding the above equation. Importantly, Eq. 66 shows that the force noise can be improved by a factor $2|t_m|^2/\mathcal{T}_2$; together with the comparative ease of realizing shot-noise-limited input light at lower powers, our approach presents a significant advantage over free-space traps.

1.5 Application: QND Measurement

Here we present the potential advantages our technique provides within the context of quantum nondemolition (QND) phonon number measurements.

1.5.1 Backaction Rate

The rate at which S_{FF} adds or removes a phonon from a mechanical oscillator containing n phonons is [1, 5]

$$\Gamma_{\mathrm{BA},n} = \frac{x_{\mathrm{ZPF}}^2}{\hbar^2}[(1+n)S_{FF}(-\Omega_{\mathrm{m}}) + nS_{FF}(+\Omega_{\mathrm{m}})]. \tag{68}$$

With a resonant drive ($\delta_+ = 0$) and in the resolved sideband regime ($\Omega_{\mathrm{m}} \gg \kappa_+$), this is

$$\Gamma_{\mathrm{BA},n} = (2n+1)x_{\mathrm{ZPF}}^2|\bar{a}_+|^2\kappa_- \frac{G_1^2G_2^2}{J^2(G_2-G_1)^2}, \tag{69}$$

where we assume $(G_2-G_1)\kappa_2/(4G_2\kappa_-) \ll \Omega_m^2/\kappa_+^2$.[2]

1.5.2 Measurement Rate

In a quadratically-coupled optomechanical system, phonons each produce a shift in the resonant frequency of the optical mode [6–8]. In a resonantly driven cavity, this will produce a shift in the phase of the reflected light. Here we derive the phonon measurement rate for an asymmetric optomechanical system with quadratic dispersive coupling using homodyne detection.

Input-Output Relations

To quantify how the phase of the reflected light depends on phonon number, we first relate the mean reflected output field $\bar{a}_1^{\mathrm{out}}$ to the mean input field $\bar{a}_1^{\mathrm{in}}$ (assuming we only address sub-cavity 1) using the standard input-output relation [1]

$$\begin{aligned}\bar{a}_1^{\mathrm{out}} &= \bar{a}_1^{\mathrm{in}} - \sqrt{\kappa_1^{\mathrm{ext}}}\bar{a}_1 \\ &= \left[1 - \tilde{\chi}_{11}(0)\kappa_1^{\mathrm{ext}}\right]\bar{a}_1^{\mathrm{in}},\end{aligned} \tag{70}$$

where $\bar{a}_1$ is the mean field in sub-cavity 1; the second line is obtained from Eq. 43. In the large gap limit, where $4J\alpha\beta \gg \kappa_1, \kappa_2, |\omega|, |\delta_+|$, which simplifies the value $\tilde{\chi}_{11}$ given by Eq. 29, this becomes

$$\begin{aligned}\bar{a}_1^{\mathrm{out}} &= \frac{i\delta_+ - \kappa_+/2 + \beta^2\kappa_1^{\mathrm{ext}}}{i\delta_+ - \kappa_+/2}\bar{a}_1^{\mathrm{in}} \\ &= Ae^{-i\phi}\bar{a}_1^{\mathrm{in}},\end{aligned} \tag{71}$$

[2] This holds, e.g., for the membrane-cavity system in the resolved sideband regime ($\Omega_m \gg \kappa_+$) in the limit $\mathcal{T}_1 \gtrsim \mathcal{T}_2$ since $(G_2-G_1)\kappa_2/(4G_2\kappa_-) = L^2\mathcal{T}_2/[4L_1^2\mathcal{T}_2 + 4L_2^2\mathcal{T}_1] \lesssim 1$.

where, in the second line, we defined the (real) amplitude reflection coefficient

$$A \equiv \sqrt{\frac{\delta_+^2 + (\beta^2\kappa_1^{\text{ext}} + \kappa_+/2)^2}{\delta_+^2 + \kappa_+^2/4}} \tag{72}$$

and the (real) reflected phase

$$\phi \equiv \arctan\left\{\frac{\delta_+\beta^2\kappa_1^{\text{ext}}}{\delta_+^2 + \kappa_+^2/4 - \beta^2\kappa_1^{\text{ext}}\kappa_+/2}\right\}. \tag{73}$$

For a resonant drive frequency ω_{in} (detuning $\delta_+ = 0$), this phase changes as

$$\left.\frac{d\phi}{d\omega_+}\right|_{\delta_+=0} = -\left.\frac{d\phi}{d\delta_+}\right|_{\delta_+=0} = \frac{-\beta^2\kappa_1^{\text{ext}}}{\kappa_+^2/4 - \beta^2\kappa_1^{\text{ext}}\kappa_+/2}, \tag{74}$$

We can also relate the mean field in the "+" mode to the input field using Eqs. 6, 43 and 44:

$$\bar{a}_+ = \frac{i\alpha J + \beta\chi_2^{-1}(0)}{J^2 + \chi_1^{-1}(0)\chi_2^{-1}(0)}\sqrt{\kappa_1^{\text{ext}}}\bar{a}_1^{\text{in}}, \tag{75}$$

so that the output field (Eq. 70) can be written in terms of "+" mode as

$$\bar{a}_1^{\text{out}} = \frac{J^2 + \chi_1^{-1}(0)\chi_2^{-1}(0) - \kappa_1^{\text{ext}}\chi_2^{-1}(0)}{i\alpha J + \beta\chi_2^{-1}(0)}\frac{\bar{a}_+}{\sqrt{\kappa_1^{\text{ext}}}}. \tag{76}$$

In the large-gap limit, this reduces to

$$\bar{a}_1^{\text{out}} = \left(\kappa_+/2 - \beta^2\kappa_1^{\text{ext}}\right)\frac{\bar{a}_+}{\sqrt{\beta^2\kappa_1^{\text{ext}}}}. \tag{77}$$

Measurement Rate with Homodyne Detection

To derive the measurement rate, we consider an ideal homodyne measurement (all the photons are collected, the laser is shot-noise limited, and the detection scheme has identical arms) where a local-oscillator ("LO"; mean optical power $\bar{P}^{\text{LO}}$) is combined at a beamsplitter with a measurement beam leaving the cavity (mean power $\bar{P}_1^{\text{out}}$) with the aim of resolving its fluctuating phase $\delta\phi(t)$. Specifically, suppose one beamsplitter input has classical LO field $E^{\text{LO}} = \sqrt{2\bar{P}^{\text{LO}}}\cos(\omega_{\text{in}}t + \Delta\phi)$ with some fixed phase $\Delta\phi$, and the other has the signal field $E_1^{\text{out}} = \sqrt{2\bar{P}_1^{\text{out}}}\cos(\omega_{\text{in}}t + \delta\phi(t))$, both oscillating at frequency ω_{in}. The homodyne signal, obtained by subtracting the photocurrents measured at each of the beamsplitter outputs, is then

$$\delta I(t) = 2A\sqrt{\bar{P}^{\text{LO}}\bar{P}_1^{\text{out}}}\sin(\delta\phi(t) - \Delta\phi), \tag{78}$$

where A is a gain relating optical power to photocurrent. Tuning the LO phase to maximize the sensitivity to phase (e.g. $\Delta\phi = 0$) and Taylor expanding sin yields

$$\delta\phi(t) \approx \left(2A\sqrt{\bar{P}_{\text{out},1}\bar{P}_{\text{LO}}}\right)^{-1} \delta I(t). \tag{79}$$

At the same time, the combined shot noise power spectral density S_{II}^{sn} from the two (subtracted) photocurrents provides a noise floor

$$S_{\phi\phi} = (4A^2\bar{P}_1^{\text{out}}\bar{P}^{\text{LO}})^{-1} S_{II}^{\text{sn}}, \tag{80}$$

and, for large LO ($\bar{P}^{\text{LO}} \gg \bar{P}_1^{\text{out}}$),

$$S_{II}^{\text{sn}} \approx A^2\hbar\omega_{\text{in}}\bar{P}^{\text{LO}}. \tag{81}$$

Furthermore, since a frequency fluctuation $\delta\omega_+$ of the cavity produces phase $\delta\phi \approx (d\phi/d\omega_+)\delta\omega_+$ ($d\phi/d\omega_+$ derived as above), the frequency noise floor

$$S_{\omega_+\omega_+} = S_{\phi\phi}\left(\frac{d\phi}{d\omega_+}\right)^{-2} = \frac{1}{4|\bar{a}_1^{\text{out}}|^2}\left(\frac{d\phi}{d\omega_+}\right)^{-2}, \tag{82}$$

where, in the last step, we substituted in Eqs. 80-81 and expressed the mean signal power $\bar{P}_1^{\text{out}} = \hbar\omega_{\text{in}}|\bar{a}_1^{\text{out}}|^2$ in term of the reflected photon rate $|\bar{a}_1^{\text{out}}|^2$, in accordance with Ref. [1].

To convert this result to the measurement time t_{meas} required to resolve a frequency shift $\Delta\omega_+$, we compare the noise floor to the frequency shift, requiring

$$t_{\text{meas}} \geq \frac{S_{\omega_+\omega_+}}{(\Delta\omega_+)^2}, \tag{83}$$

in order to resolve the frequency shift with unity signal-to-noise ratio. For a single phonon jump, the induced frequency shift is

$$\Delta\omega_+ = \frac{d^2\omega_+}{dx^2}x_{\text{ZPF}}^2, \tag{84}$$

yielding a measurement rate

$$\Gamma_{\text{meas}} \equiv \frac{1}{t_{\text{meas}}} = 4|\bar{a}_1^{\text{out}}|^2\left(\frac{d\phi}{d\omega_+}\frac{d^2\omega_+}{dx^2}x_{\text{ZPF}}^2\right)^2. \tag{85}$$

In the large gap limit, using Eq. 12 for $d^2\omega_+/dx^2$, and Eqs. 74 and 77 derived in Sec. 1.5.2 to substitute $d\phi/d\omega_+$ and $\bar{a}_{\text{out},1}$ respectively, this measurement rate simplifies to

$$\Gamma_{\text{meas}} = \frac{16|\bar{a}_+|^2}{\kappa_+}\frac{\beta^2\kappa_1^{\text{ext}}}{\kappa_+}\left(\frac{d^2\omega_+}{dx^2}x_{\text{ZPF}}^2\right)^2 \tag{86}$$

$$= \frac{64|\bar{a}_+|^2}{\kappa_+}\frac{\beta^2\kappa_1^{\text{ext}}}{\kappa_+}\frac{1}{J^2}\frac{(-G_1G_2)^3}{(G_2-G_1)^2}x_{\text{ZPF}}^4. \tag{87}$$

The correction term $\beta^2\kappa_1^{\text{in}}/\kappa_+$ accounts for the proportion of photons in the "+" mode leaving through the input port.

For the case of a truly single-port cavity ($\kappa_2 = 0$ and $\kappa_1 = \kappa_1^{\text{ext}}$), the measurement rate is

$$\begin{aligned}\Gamma_{\text{meas}} &= \frac{16|\bar{a}_+|^2}{\kappa_+}\left(\frac{d^2\omega_+}{dx^2}x_{\text{ZPF}}^2\right)^2 \\ &= \frac{64|\bar{a}_+|^2}{\kappa_+}\frac{(-G_1G_2)^3}{J^2(G_2-G_1)^2}x_{\text{ZPF}}^4.\end{aligned} \tag{88}$$

Note for a membrane-cavity system, κ_+, $\partial_x^2\omega_+$, and thus Γ_{meas}, do not depend upon at which quadratic point the membrane is positioned, allowing one to tune the ratio G_1/G_2 without affecting the measurement rate.

1.5.3 Backaction-Limited Number State Resolution

The measurement rate, which is derived in Sec. 1.5.2 above, is

$$\Gamma_{\text{meas}} = \frac{64|\bar{a}_+|^2}{\kappa_+}\frac{\beta^2\kappa_1^{\text{ext}}}{\kappa_+}\frac{1}{J^2}\frac{(-G_1G_2)^3}{(G_2-G_1)^2}x_{\text{ZPF}}^4, \tag{89}$$

yielding a figure of merit

$$\frac{\Gamma_{\text{meas}}}{\Gamma_{\text{BA},n}} = \frac{64}{2n+1}\frac{g_1g_2}{\kappa_-\kappa_+}\frac{\beta^2\kappa_1^{\text{ext}}}{\kappa_+}, \tag{90}$$

describing how well a phonon number state n can be measured before backaction causes a jump, where we define the usual optomechanical coupling rate $g_i \equiv x_{\text{ZPF}}|G_i|$. In the single-port cavity limit ($\kappa_2 = 0$), this ratio becomes

$$\frac{\Gamma_{\text{meas}}}{\Gamma_{\text{BA},n}} = \frac{64}{2n+1}\frac{(g_2+g_1)^2}{\kappa_1^2} = \frac{64}{2n+1}\frac{g_2^2}{\kappa_+^2}. \tag{91}$$

The advantage of our approach becomes clearer if we consider a membrane-cavity system in which the membrane is a distance L_1 from the first mirror and L_2 from the second (total length $L = L_1+L_2$). If the sub-cavity crossing frequency $\omega_0 = N_1\pi c/L_1 = N_2\pi c/L_2$ where $N_i = 2L_i/\lambda$ is the (integer) mode index of each sub-cavity at wavelength λ, and the coupling rates $G_1 = -\omega_0/L_1$ and $G_2 = +\omega_0/L_2$, the ratio becomes

$$\begin{aligned}\frac{\Gamma_{\text{meas}}}{\Gamma_{\text{BA},n}} &= \frac{64}{2n+1}\left(\frac{\omega_0 x_{\text{ZPF}}}{L_2\kappa_0}\right)^2 \\ &= \frac{64}{2n+1}\left(\frac{g_{\text{MIM}}}{\kappa_0}\right)^2\left(\frac{L}{2L_2}\right)^2\end{aligned} \tag{92}$$

with κ_0 being the empty cavity power decay rate (Eq. 18). The second line is expressed in terms of the half-cavity single-photon optomechanical coupling rate for the MIM

system $g_{\mathrm{MIM}} \equiv 2x_{\mathrm{ZPF}}\omega_0/L$ to facilitate a direct comparison: by reducing L_2 (moving the membrane toward the back mirror), the usual strong coupling requirement $g_{\mathrm{MIM}}/\kappa_0 > 1$ for measuring a state before QRFN destroys it [2] is relaxed by a factor $L/2L_2$, which can be as large as $\sim L/\lambda$ at the quadratic point nearest the back mirror.

For fixed mirror losses (round trip power loss $\mathcal{L}_j = \mathcal{L}$, say) we can improve the fidelity by a less dramatic factor, and there is some advantage to be gained by bringing $|t_1|^2$ closer to $\mathcal{L}$. To calculate the optimal $L_{1,\mathrm{min}}$ and $t_{1,\mathrm{opt}}$, we first substitute the expression for the decay rates (Eqs. 18 and 19), and optomechanical coupling $g_i = x_{\mathrm{ZPF}}\omega_0/L_j$ in the ratio Eq. 90; the optimal membrane position is then

$$L_{1,\mathrm{min}} = \frac{\mathcal{T}_1}{\mathcal{T}_1 + \mathcal{T}_2} L \tag{93}$$

where the force noise is minimal and the ratio

$$\left.\frac{\Gamma_{\mathrm{meas}}}{\Gamma_{\mathrm{BA},n}}\right|_{L_{1,\mathrm{min}}} = \frac{256}{2n+1}\frac{\omega_0^2 x_{\mathrm{ZPF}}^2}{c^2}\frac{|t_1|^2}{\mathcal{T}_1\mathcal{T}_2(\mathcal{T}_1+\mathcal{T}_2)}, \tag{94}$$

is maximal; $L_{1,\mathrm{min}}$ is the same as before (Eq. 57) since the measurement rate is independent of the membrane position within the cavity. We can also compare with the same ratio for the membrane-in-the-middle,

$$\left.\frac{\Gamma_{\mathrm{meas}}}{\Gamma_{\mathrm{BA},n}}\right|_{L/2} = \frac{1024}{2n+1}\frac{\omega_0^2 x_{\mathrm{ZPF}}^2}{c^2}\frac{|t_1|^2}{(\mathcal{T}_1+\mathcal{T}_2)^3}, \tag{95}$$

finding our approach yields an improvement

$$\left.\frac{\Gamma_{\mathrm{meas}}}{\Gamma_{\mathrm{BA},n}}\right|_{L_{1,\mathrm{min}}} \Bigg/ \left.\frac{\Gamma_{\mathrm{meas}}}{\Gamma_{\mathrm{BA},n}}\right|_{L/2} = \frac{1}{4}\frac{(\mathcal{T}_1+\mathcal{T}_2)^2}{\mathcal{T}_1\mathcal{T}_2} \to \frac{1}{4}\frac{|t_1|^2}{\mathcal{T}_2}. \tag{96}$$

As expected, this is the same improvement as we found for the force noise.

With the membrane at the optimal $L_{1,\mathrm{min}}$, we can also calculate the the optimal input mirror transmission

$$|t_1|^2_{\mathrm{opt}} = \sqrt{\mathcal{L}_1(|t_2|^2 + \mathcal{L}_1 + \mathcal{L}_2)}, \tag{97}$$

that maximizes the ratio, yielding

$$\left.\frac{\Gamma_{\mathrm{meas}}}{\Gamma_{\mathrm{BA},n}}\right|_{L_{1,\mathrm{min}},|t_1|^2_{\mathrm{opt}}} = \frac{256}{2n+1}\frac{\omega_0^2 x_{\mathrm{ZPF}}^2}{c^2}\frac{|t_2|^2 + 2\mathcal{L}_1 + \mathcal{L}_2 - 2\sqrt{\mathcal{L}_1(|t_2|^2+\mathcal{L}_1+\mathcal{L}_2)}}{(|t_2|^2+\mathcal{L}_2)^3}. \tag{98}$$

This optimized QND "fidelity" is a factor (for $\mathcal{L}_j = \mathcal{L}$)

$$\left.\frac{\Gamma_{\mathrm{meas}}}{\Gamma_{\mathrm{BA},n}}\right|_{L_{1,\mathrm{min}},|t_1|^2_{\mathrm{opt}}} \Bigg/ \left.\frac{\Gamma_{\mathrm{meas}}}{\Gamma_{\mathrm{BA},n}}\right|_{L_{1,\mathrm{min}},\mathrm{matched}} = 2 + 6\frac{\mathcal{L}}{|t_2|^2} - 4\sqrt{\frac{\mathcal{L}}{|t_2|^2}\left(1 + 2\frac{\mathcal{L}}{|t_2|^2}\right)} \tag{99}$$

larger than that of a traditional matched cavity ($|t_1|$ set equal to $|t_2|$). Equation 99 can be viewed as a prefactor that generalizes the existing "standard quantum limit" [9] to the case of asymmetric systems. The largest gains occur in systems maximing the back-mirror reflectivity, which is just a statement that one needs to open the input mirror enough to get a reasonable fraction of the cavity light out, and up to 3 dB improvement can also be achieved with transmission-dominated mirrors ($\mathcal{T} \ll |t_j|^2$), though this assumes we ignore the information in the light leaving the back mirror.

For a fair comparison with MIM systems, it is also possible to calculate the optimal transmission

$$|t_1|^2_{\mathrm{MIM}} = (|t_2|^2 + \mathcal{L}_1 + \mathcal{L}_2)/2 \tag{100}$$

maximizing the measurement rate to backaction rate ratio for the membrane-in-the middle (Eq. 95), yielding a ratio

$$\left.\frac{\Gamma_{\mathrm{meas}}}{\Gamma_{\mathrm{BA},n}}\right|_{L/2,|t_1|^2_{\mathrm{MIM}}} = \frac{4096}{27(2n+1)}\frac{\omega_0^2 x_{\mathrm{ZPF}}^2}{c^2}\frac{1}{(|t_2|^2+\mathcal{L}_1+\mathcal{L}_2)^2}, \tag{101}$$

and which is a factor

$$\frac{\left.\frac{\Gamma_{\mathrm{meas}}}{\Gamma_{\mathrm{BA},n}}\right|_{L_{1,\min},|t_1|^2_{\mathrm{opt}}}}{\left.\frac{\Gamma_{\mathrm{meas}}}{\Gamma_{\mathrm{BA},n}}\right|_{L/2,|t_1|^2_{\mathrm{MIM}}}} = \frac{27}{16}\frac{(|t_2|^2+\mathcal{L}_1+\mathcal{L}_2)^2(|t_2|^2+2\mathcal{L}_1+\mathcal{L}_2-2\sqrt{\mathcal{L}_1(|t_2|^2+\mathcal{L}_1+\mathcal{L}_2)})}{(|t_2|^2+\mathcal{L}_2)^3} \tag{102}$$

lower than at the optimal membrane position.

2 Hopping Rate for a Membrane-in-Cavity

In this section, we derive the classical equations of motion for the electric fields for a cavity with a membrane inside it, extending the formalism of Refs. [10–12]. This allows for a simple derivation of EOMs and direct access to the hopping rate J between two sub-cavities separated by a partial reflector.

Consider the Fabry-Perot cavity in Fig. 1, comprising two end mirrors of field reflection (transmission) coefficients r_j (t_j) partitioned by a third mirror (membrane) having field reflection (transmission) coefficient r_m (t_m), such that the sub-cavity lengths L_j sum to total length $L = L_1 + L_2$. The right-moving field amplitude A_2 just to the right of the membrane at a time t is related to the left and right incoming amplitudes A_1 and B_2 as

$$A_2(t) = r_m B_2(t) + t_m A_1(t), \tag{103}$$

Following this wave a round-trip time $\tau_2 = 2L_2/c$ later in sub-cavity 2 (c is the speed of light), we find a returning field

$$B_2(t+\tau_2) = r_2 e^{i\omega_{\mathrm{in}}\tau_2} A_2(t), \tag{104}$$

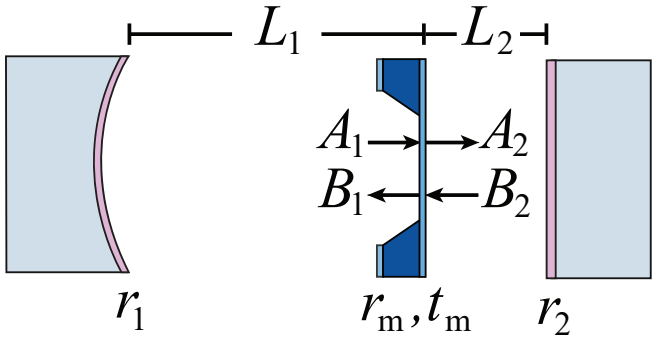

Figure 1: A Fabry-Pérot cavity comprising a left-hand and right-hand mirror with field reflection coefficients r_1 and r_2, split into two sub-cavities of length L_1 and L_2 by a membrane with field reflection (transmission) coefficients r_m (t_m). A_j indicate the right moving fields and B_j the left moving fields just outside the membrane surfaces.

in a frame rotating at the laser frequency $\omega_{\rm in}$. Substituting Eq. 103 in Eq. 104, we obtain

$$B_2(t+\tau_2) = r_m r_2 e^{i\omega_{\rm in}\tau_2} B_2(t) + t_m r_2 e^{i\omega_{\rm in}\tau_2} A_1(t) \tag{105}$$

For small τ_2[3], we can approximate the time derivative of B_2 as

$$\begin{aligned}\dot{B}_2(t) &\approx \frac{B_2(t+\tau_2) - B_2(t)}{\tau_2} \\ &= -\frac{1 - r_2 r_m e^{i\omega_{\rm in}\tau_2}}{\tau_2} B_2(t) + \frac{t_m r_2 e^{i\omega_{\rm in}\tau_2}}{\tau_2} A_1(t).\end{aligned} \tag{106}$$

Following the same method for the left sub-cavity field, we find

$$\dot{A}_1(t) \approx -\frac{(1 - r_m r_1 e^{i\omega_{\rm in}\tau_1})}{\tau_1} A_1(t) + \frac{t_m r_1 e^{i\omega_{\rm in}\tau_1}}{\tau_1} B_2(t). \tag{107}$$

As a matter of convention, we then rescale the fields as

$$\alpha_1(t) = -\sqrt{L_1} A_1(t) \tag{108}$$

$$\alpha_2(t) = +\sqrt{L_2} B_2(t) \tag{109}$$

such that $|\alpha_j|^2$ represents the number of photons in sub-cavity j. In a matrix form, these coupled equations then become

$$\begin{pmatrix}\dot{\alpha}_1(t) \\ \dot{\alpha}_2(t)\end{pmatrix} = \begin{pmatrix} -\frac{c}{2L_1}(1 - r_1 r_m e^{i\omega_{\rm in}\tau_1}) & \frac{-r_1 e^{i\omega_{\rm in}\tau_1} c t_m}{2\sqrt{L_1 L_2}} \\ \frac{-r_2 e^{i\omega_{\rm in}\tau_2} c t_m}{2\sqrt{L_1 L_2}} & -\frac{c}{2L_2}(1 - r_2 r_m e^{i\omega_{\rm in}\tau_2}) \end{pmatrix} \begin{pmatrix}\alpha_1(t) \\ \alpha_2(t)\end{pmatrix}, \tag{110}$$

[3]We assume the round trip time is small compared to the other relevant time-scales of the system, such that A_j and B_j are slowly varying. Specifically, $1/\tau_2 \gg \kappa_1, \kappa_2, \Omega_{\rm m}, J$; the first two conditions arise from $|t_1|, |t_2| \ll 1$ and the last one arises from $|t_m| \ll \sqrt{L_1/L_2}$.

in agreement with the more careful derivation of Ref. [13].

To recover the equations obtained from input-output theory, we make additional approximations. First, for simplicity, we now make a common unitarity preserving choice for the phase on all the coefficients, such that $r_m = -|r_m|$ and $t_m = i|t_m|$. We furthermore assume that the end mirrors have high reflectivity such that $r_j \approx -1 + |t_j|^2/2$, and write the laser frequency as

$$\omega_{\text{in}} = \Delta + \omega_j(\Delta x) - G_j \Delta x, \tag{111}$$

where $\Delta \equiv \omega_{\text{in}} - \omega_0$ is the detuning from the crossing frequency (defining $\Delta x \equiv 0$), $\omega_j(\Delta x)$ is the resonant frequency of sub-cavity j, and $G_j = \partial_x \omega_j$ is the usual linear dispersive coupling. Note that, by definition, the sub cavities have an integer $N_j = 2L/\lambda_j$ half wavelengths, such that $\omega_j(\Delta x)\tau_j = 2\pi N_j$. Again assuming that the detuning is much smaller than the round-trip rate of each sub-cavity ($|\Delta| \sim \kappa_j \ll 1/\tau_j$), that the membrane is displaced by much less than a half wavelength ($\Delta x \ll \lambda/2$, or, equivalently, $|G_j \Delta x| \ll 1/\tau_j$), and keeping only the terms to leading order in $|t_m|$, $|t_1|^2$, $|t_2|^2$, and Δ,

$$\begin{pmatrix} \dot{\alpha}_1(t) \\ \dot{\alpha}_2(t) \end{pmatrix} = \begin{pmatrix} i(\Delta - G_1\Delta x) - \kappa_1/2 & i\frac{c|t_m|}{2\sqrt{L_1 L_2}} \\ i\frac{c|t_m|}{2\sqrt{L_1 L_2}} & i(\Delta - G_2\Delta x) - \kappa_2/2 \end{pmatrix} \begin{pmatrix} \alpha_1(t) \\ \alpha_2(t) \end{pmatrix}, \tag{112}$$

with $\kappa_j = c|t_j|^2/(2L_j)$. Most importantly, we can immediately identify the off-diagonal elements as the hopping rate

$$J = \frac{c|t_m|}{2\sqrt{L_1 L_2}} = \frac{c|t_m|\sqrt{-G_1 G_2}}{2\omega_0}. \tag{113}$$

References

[1] A. A. Clerk, M. Devoret, S. Girvin, F. Marquardt, and R. Schoelkopf, "Introduction to quantum noise, measurement and amplification," Rev. Modern Phys. **82**, 1155 (2010).

[2] Y. Yanay, J. Sankey, and A. A. Clerk, "Quantum backaction and noise interference in asymmetric two-cavity optomechanical systems," Phys. Rev. A **93**, 063809 (2016).

[3] F. Elste, S. Girvin, and A. A. Clerk, "Quantum noise interference and backaction cooling in cavity nanomechanics," Phys. Rev. Lett. **102**, 207209 (2009).

[4] K. Ni, R. Norte, D. Wilson, J. Hood, D. Chang, O. Painter, and H. Kimble, "Enhancement of mechanical q factors by optical trapping," Phys. Rev. Lett. **108**, 214302 (2012).

[5] A. A. Clerk, F. Marquardt, and J. Harris, "Quantum measurement of phonon shot noise," Phys. Rev. Lett. **104**, 213603 (2010).

[6] J. Thompson, B. Zwickl, A. Jayich, F. Marquardt, S. Girvin, and J. Harris, "Strong dispersive coupling of a high-finesse cavity to a micromechanical membrane," Nature **452**, 72 (2008).

[7] A. Jayich, J. Sankey, B. Zwickl, C. Yang, J. Thompson, S. Girvin, A. A. Clerk, F. Marquardt, and J. Harris, "Dispersive optomechanics: a membrane inside a cavity," New J. Phys. **10**, 095008 (2008).

[8] M. Bhattacharya, H. Uys, and P. Meystre, "Optomechanical trapping and cooling of partially reflective mirrors," Phys. Rev. A **77**, 033819 (2008).

[9] H. Miao, S. Danilishin, T. Corbitt, and Y. Chen, "Standard quantum limit for probing mechanical energy quantization," Phys. Rev. Lett. **103**, 100402 (2009).

[10] M. Lawrence, B. Willke, M. Husman, E. Gustafson, and R. Byer, "Dynamic response of a fabry-perot interferometer," J. Optical Society America B **16**, 523 (1999).

[11] D. Wilson, *Cavity Optomechanics with High-Stress Silicon Nitride Films*, Ph.D. thesis, California Institute of Technology (2011).

[12] M. Rakhmanov, *Dynamics of Laser Interferometric Gravitational Wave Detectors*, Ph.D. thesis, California Institute of Technology (2000).

[13] R. J. Lang and A. Yariv, "Local-field rate equations for coupled optical resonators," Phys. Rev. A **34**, 2038 (1986).